Comparison of Upper Neck Loads of the Large Omni-Directional Child ATD to Pediatric Volunteers in Low-Speed Sled Tests

Baker G[1,2], Stammen JA[3], Suntay B[4] Arbogast KB[1,5], Seacrist T[1]

1. *Center for Injury Research and Prevention, Children's Hospital of Philadelphia*
2. *Department of Mechanical Engineering, University of Kansas*
3. *Vehicle Research and Testing, National Highway Traffic Safety Administration*
4. *Transportation Research Center Inc.*
5. *Perelman School of Medicine, University of Pennsylvania*

ABSTRACT

Motor vehicle crashes are the leading cause of pediatric mortality and injury, with head injuries as the most common. To better mitigate these injuries, pediatric ATDs must mimic pediatric motion and internal forces as well as accurately predict injury potential during a crash. Previous studies of pediatric ATDs have shown an overestimation of upper neck loads and injury risk due to limited biofidelity of the ATDs. Recently, a large omni-directional child ATD has been developed in an effort to improve biofidelity through a more realistic shoulder construction, softer cervicothoracic junction, and a multi-segmented, more flexible thoracic spine compared to the Hybrid III 10. This study sought to evaluate the influence of these modifications on LODC neck loading by comparing its response to previously collected child volunteer data in low-speed frontal sled tests.

Low-speed (<4g) frontal sled tests were conducted with the LODC. The LODC was restrained using a 3-point belt. Photo-reflective targets were placed on important anatomic landmarks, such as head top, and were captured using a 3D near infrared tracking system. Variables considered were shear force (F_x), axial force (F_z), and bending moment (M_y) about the upper neck. These parameters were calculated using standard equations of motion. This data is compared to previous data from 9-11 year old pediatric volunteers, the Hybrid III 10, and the Q10 that were tested utilizing similar methods.

The LODC significantly underestimated mean shear force (LODC = -98 N; HIII 10 = -138 N; Q10 = -151 N; Volunteers = -132 N) compared to the HIII 10, Q10 and volunteers. The LODC also underestimated axial force compared to the volunteers (LODC = 41 N; Volunteers = 67 N) yet was closer to volunteer levels than both the HIII 10 and Q10 (HIII 10 = 15 N; Q10 = 13 N). These differences are likely due to the LODC's greater flexibility, especially in the thoracic region of the spine. A shift in force distribution from shear to axial is displayed, likely due to greater head rotation displayed by the LODC than the HII 10 or Q10 ATDs. These data provide valuable information on the biofidelity of the recently developed LODC.

INTRODUCTION

Motor vehicle crashes (MVCs) are the leading cause of unintentional injury deaths in the United States for children aged 5 – 18 years (Centers for Disease Control 2013). Of injuries sustained by children in MVCs, head injuries are the most common (Arbogast et al. 2005). Decreasing the prevalence of these injuries stems from better understanding of the motion and forces of adolescent passengers sustained during motor vehicle crashes. With a lack of supply and social controversy surrounding use of pediatric post mortem human subjects (PMHS) to gain this understanding, pediatric ATDs validated by human volunteer data are integral to gaining a better understanding of how to prevent adolescent injury and death caused by motor vehicle crashes.

Human volunteer data has been successfully used as comparison to evaluate ATDs for both adults and adolescents (Begeman et al. 2012; Seacrist, Mathews et al. 2012; Seacrist et al. 2013, 2014). Use of adolescent human volunteer data in the development of these pediatric ATDs has allowed comparison of the motion and loading experienced by adolescents to better quantify the biofidelity of these pediatric ATDs. Pediatric ATD response corridors were previously scaled from adult biomechanical data (Irwin and Mertz 1997). Adolescent human volunteer data provides a better comparison than the previously utilized scaled adult biomechanical data as human volunteer comparison better accounts for differences in spinal maturity seen between adolescents and adults.

Several pediatric ATDs have been developed to help understand how children respond to impact scenarios. The Hybrid III and the Q Series ATDs both provided important insight to the responses of children in frontal and side impacts. Previous studies have compared the responses of pediatric volunteers to the Hybrid III and Q Series ATDs (Seacrist et al. 2010, 2013; Seacrist, Mathews, et al. 2012). However, these ATDs presented limited biofidelity as they displayed reduced excursions, increased belt loading, and increased upper neck bending moments compared to the human volunteers. Previous research has also raised concerns of the chin-to-chest contact displayed by the Hybrid III ATDs (Menon et al. 2004, 2005; Stammen et al. 2012) that was inconsistent with injury data (NHTSA 20120-0158-0001). This overestimation of neck loads and injury risk can be attributed to the lack of biofidelity in the neck and spine construction of the Hybrid III.

In an attempt to better mitigate these injuries, pediatric ATDs must mimic pediatric motion and internal forces as well as accurately predict injury potential during a crash. Recently, a large omni-directional child (LODC) ATD has been developed in an ongoing effort to improve biofidelity of pediatric ATDs. Specifically, the LODC made improvements to biofidelity by lengthening the neck and incorporating a softer cervicothoracic junction (junction of C7 and T1 vertebrae) than the Hybrid III 10. The LODC also implemented a more realistic shoulder construction by implementing a ball joint for the shoulder and a plastic scapula and clavicle with flexible attachments. The LODC introduced flexible spine elements between each rigid spine segment to better model pediatric spine movement. The rib shape of the LODC also matches child anthropometry and has a rigid sternum with flexible attachment to the ribs.

This study sought to further evaluate the influence of these modifications on the biofiedlity of the LODC. Neck loading of the LODC was evaluated by comparing its response to previously collected 9-11 year old human volunteer data in low-speed sled tests.

2

METHODS

A comprehensive description of methods can be found in Abrogast et al. (2009). To compare to previous data from 9-11 year old pediatric volunteers (n=7), the Hybrid III 10, and the Q10, the same methods were utilized for all human subjects and ATDs, including the new LODC.

Briefly, low-speed sled tests were conducted with the LODC using a pneumatically actuated, hydraulically controlled low-speed deceleration sled equipped with an onboard accelerometer. A safe, noninjurous crash pulse (<4g) was applied to the sled. This impulse was derived from an amusement park bumper car impact applicable to adolescents. The LODC was restrained using a standard 3-point belt used in automotive systems (Takata Corp., Tokyo, Japan). Lightweight belt load cells (model 6200FL-41-30, Denton ATD Inc., Rochester Hills, MI) were attached to the shoulder belt on the right and left locations on the lap belt. The belt geometry ensured that the D-ring was located 296 mm reward of the H-point, inside of the measured range of 2001-2008 U.S.-based vehicles (Reed et al. 2008). Lightweight belt webbing load cells (model 6200FL-41-30, Denton ATD Inc., Rochester Hills, MI) were attached to the shoulder belt on the right and left locations on the lab belt. Torso and knee angles were initially positioned to 110°. The shoulder belt anchor height was adjusted to provide a similar fit LODC to the previously tested human subjects. The angle the shoulder belt makes with horizontal was initially set at 55° (as measured by an inclinometer) by raising or lowering the D-ring. The lap belt anchor locations were fixed at 55° throughout the test series.

Photo-reflective targets were placed on important anatomic landmarks, such as head top, C4, T1, external auditory meatus (bilaterally), suprasternal notch, and xiphoid process, and were captured using an 8-camera 3D near-infrared tracking system (model Eagle 4, Motion Analysis Corporation, Santa Rosa, CA). This video tracking system captured the motion of these photo-reflective targets by combining the 2D images from each camera and the intensity of the marker reflection. Accuracy was verified by a static and dynamic calibration procedure that revolved a 500-mm calibration distance to 0.1 mm. The LODC underwent six repetitive trials of low-speed frontal impact.

Load cells and accelerometer were sampled at 10,000 Hz using a T-DAS data acquisition system (Diversified Technical Systems Inc., Seal Beach, CA) with a built-in anti-aliasing filter (4,300 Hz). Sled acceleration, seat belt loads, and forces and moments at the seat pan and footrest were filtered at SAE channel frequency class 60, according to SAE J211 (Society of Automotive Engineers 1995). Motion data analysis data were acquired at 100 Hz, which provided the optimal sampling frequency and resolution for this test series, and analyzed using Motion Analysis Cortex 2.5 software (Motion Analysis Corporation, Santa Rosa, CA). High-speed video was collected at 1,000 Hz.

The LODC data were compared to the Hybrid III 10, Q10, and previously collected 9-11 year old pediatric volunteer data. To account for variations in stature and mass within the age groups, trajectories and seat environment reaction loads of the volunteers and Q-series ATDs were scaled to the anthropometry of the corresponding Hybrid III ATD according to length scaling (Eq. 1) (Langhaar 1951) and force scaling (Eq. 2) (Eppinger et al. 1984), respectively:

$$\lambda_L = \frac{L_{Hybrid\,III}}{L_{subject}} \tag{1}$$

3

$$\lambda_F = \lambda_m^{2/3} = \left(\frac{m_{Hybrid\,III}}{m_{subject}}\right)^{2/3} \tag{2}$$

The T-DAS and motion analysis data were imported in MATLAB (Mathworks, Inc., Natick, MA) for analysis using a custom algorithm. The origin of the local (sled) coordinate system was determined as the right rear seat pan marker. Head and neck markers were used to compute peak excursion relative to event onset.

The primary variables considered were shear force (F_x), axial force (F_z), and bending moment (M_y) about the upper neck. A comprehensive description of the inverse dynamics methods can be found in Seacrist et al. (2012). Head angle was determined as the angle of the vector from the midpoint of the bilateral external auditory meatus markers (mEAM) to the nasion relative to the ground. This vector was angled upward from relative to the neutral head axis, and as such, was subtracted from the head vector angle across time to obtain a neutral axis head angle. This neutral head angle was then differentiated to obtain angular velocity ($\dot{\theta}_{head}$) and angular acceleration ($\ddot{\theta}_{head}$). Linear acceleration of the head ($\ddot{x}_{mEAM}, \ddot{z}_{mEAM}$) was obtained by twice differentiating the 3D position of the mEAM in the laboratory coordinate system. A second order low pass Butterworth filter with a 25 Hz cutoff frequency was used to smooth the linear and angular terms after each differentiation. The mEAM accelerations were rotated from the global (lab) to the local (head) coordinate system, then transformed from the mEAM to the head center of gravity (CG) using standard rigid body dynamics equations (Eq. 3):

$$\begin{bmatrix} \ddot{x}_{CG} \\ \ddot{z}_{CG} \end{bmatrix} = \begin{bmatrix} \ddot{x}_{mEAM} \\ \ddot{z}_{mEAM} \end{bmatrix} + \begin{bmatrix} \rho_z \\ -\rho_x \end{bmatrix} \ddot{\theta}_{head} - \begin{bmatrix} \rho_x \\ \rho_z \end{bmatrix} \dot{\theta}_{head}^2 \tag{3}$$

where ρ is the vector from the mEAM to the CG in the head coordinate system. Shear force (F_x), axial force (F_z) (Eq. 4), and bending moment (M_y) (Eq. 5) were calculated about the upper neck using standard equations of motion:

$$\sum F_{OC} : \begin{bmatrix} F_x \\ F_z \end{bmatrix} = m_{head} \begin{bmatrix} \ddot{x}_{CG} \\ \ddot{z}_{CG} \end{bmatrix} - m_{head} \begin{bmatrix} g \sin \varphi \\ g \cos \varphi \end{bmatrix} \tag{4}$$

$$\sum M_{CG} : M_y = I_{yy} \ddot{\theta}_{head} - F_x d_z - F_z d_x \tag{5}$$

where m_{head} is the mass of the head, I_{yy} is the moment of inertia about the y-axis, and d_x and d_z are scalar distances from the CG to the occipital condyles (OC) in the head coordinate system. The neck injury criterion was also calculated (Eqn. 6):

$$N_{ij} = \frac{|F_z|}{F_{int}} + \frac{|M_y|}{M_{int}} \tag{6}$$

where F_z is the axial force, M_y is the bending moment, F_{int} and M_{int} represent the ATD-specific critical intercept values used for normalized N_{ij}, *i* represents compression/tension, and *j* represents flexion/extension. This criterion assesses injury risk to living humans based off of the ATD data.

4

RESULTS

The time histories of shear force, axial force, and bending moment are shown in Figs. 1, 2, 3, respectively. Mean (±SE) peak $\ddot{x}_{CG}$, $\ddot{z}_{CG}$, F_x, F_z, M_y, $\ddot{\theta}_{head}$, and N_{ij} for the LODC compared to the HIII, Q10, and human volunteers are listed in Table 1. Compared to the matched volunteer cohorts, the LODC significantly underestimated upper neck shear force in contrast to the Q10's overestimation of shear. The LODC also underestimated axial force compared to the volunteers yet was closer to volunteer levels than both the HIII 10 and Q10. Similar to the HIII 10, the LODC underestimated upper neck bending moment compared to the volunteers while the Q10 overestimated bending moment. Again similar to the HIII 10, the LODC also underestimated the neck injury criterion while the Q10 overestimated compared to the human volunteers. All ATDs underestimated the peak head angular acceleration during flexion compared to the volunteers, but the LODC was closer to volunteer levels than the HIII 10 and Q10. The LODC also substantially overestimated $\ddot{x}_{CG}$ and $\ddot{z}_{CG}$ while the HIII and Q10 presented closer results to the volunteers. The LODC exhibited later times to peak response for shear force, axial force, and bending moment in contrast to the HIII 10 and Q10 which tended to have quicker response times. In contrast, the LODC's response time to peak angular head acceleration was quicker than the volunteers yet closer than the HIII 10 and Q10 response times.
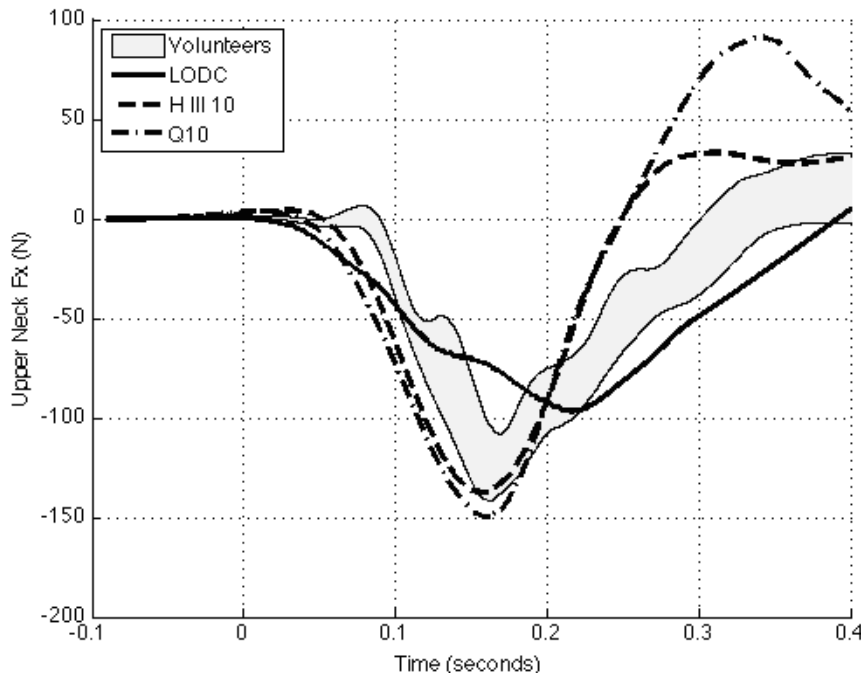

Figure 1: Average time-series responses of F_x of ATDs compared to 95% CI volunteer envelope. Time zero represents the onset of sled acceleration. Positive values indicate posterior shear; negative values indicate anterior shear.
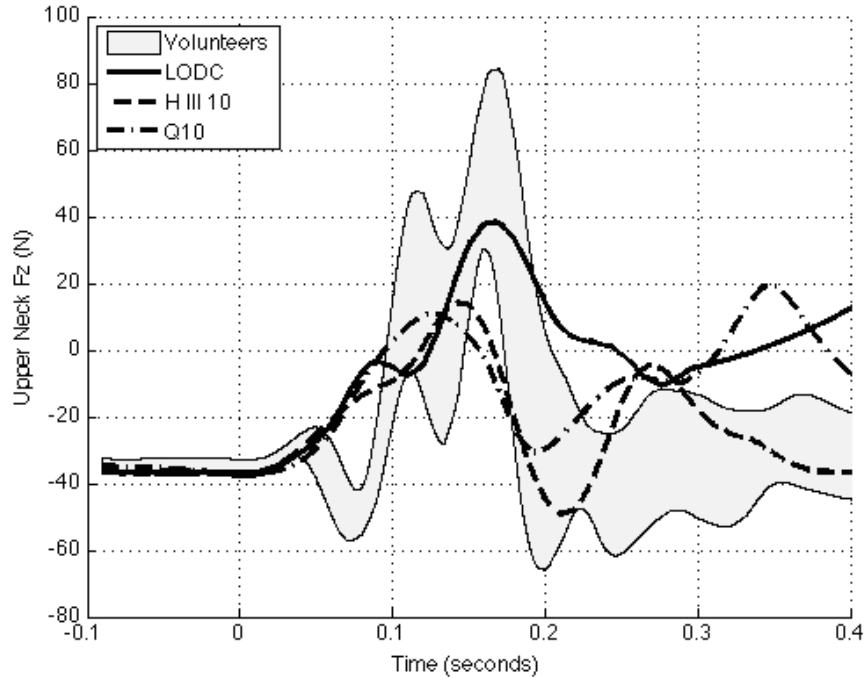
Figure 2: Average time-series responses of F_z of ATDs compared to 95% CI volunteer envelope. Time zero represents the onset of sled acceleration. Positive values indicate tension; negative values indicate compression.
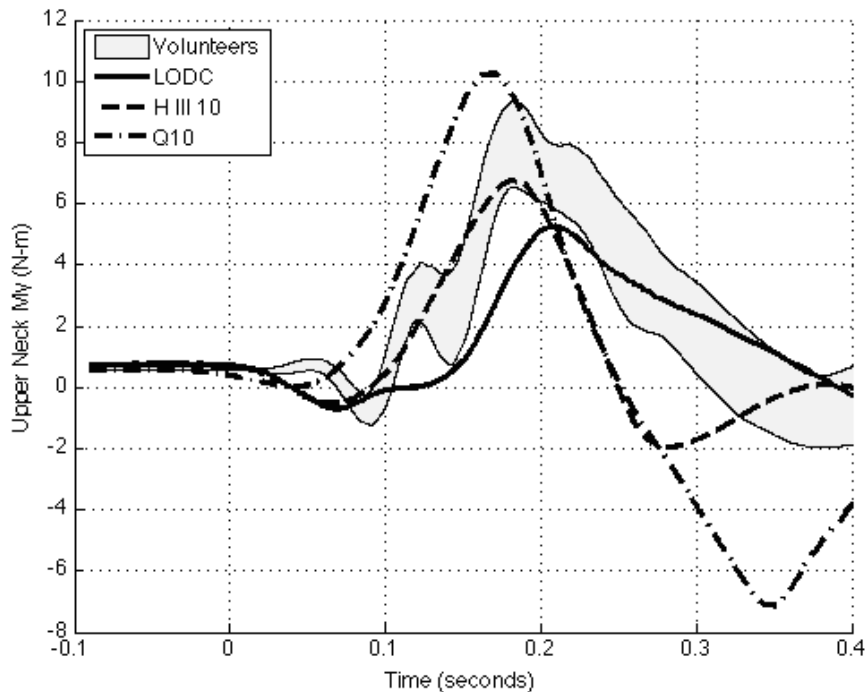

Figure 3: Average time-series responses of M_y of ATDs compared to 95% CI volunteer envelope. Time zero represents the onset of sled acceleration. Positive values indicate flexion; negative values indicate extension.

Table 1: Peak Upper neck loads

	LODC mean (±SE)	HIII 10 mean (±SE)	Q10 mean (±SE)	Human volunteers 95% CI		
				Lower	Mean	Upper
F_x						
Peak (N)	-97.6 ± 2.4*	-138 ± 2	-151 ± 3*	-122	-132	-142
Time (ms)	210 ± 8*	159 ± 2	160 ± 3	159	167	171
F_z						
Peak (N)	40.9 ± 4.9*	15 ± 5*	13 ± 4*	50	67	84
Time (ms)	165 ± 5	145 ± 2*	133 ± 6*	146	155	165
M_y						
Peak (N m)	5.4 ± 0.3*	6.8 ±0.3*	10.4 ± 0.3*	7.8	8.6	9.5
Time (ms)	211 ± 4*	182 ± 2	172 ± 4*	180	194	208
θ''_{head}						
Peak (rad/s^2)	-128.4 ± 12.4*	-90 ± 5*	-88 ± 5*	-130	-163	-195
Time (ms)	106 ± 13*	92 ± 3*	80 ± 5*	141	145	150
x''_{CG}						
Peak (m/s^2)	-17.7 ± 0.5*	-3.3 ± 0.1	-3.8 ± 0.2*	-3.1	-3.5	-3.8
z''_{CG}						
Peak (m/s^2)	8 ± 1.3*	0.3 ± 0.3*	0.4 ± 0.2*	1.4	1.9	2.3
N_{ij}	0.1 ± 0.01*	0.13 ± 0.00*	0.19 ± 0.00*	0.15	0.17	0.18

*Significant differences (p<0.05) between ATD and human volunteers.

DISCUSSION

This study sought to further analyze the biofidelity of pediatric ATDs by evaluating the improved LODC ATD in low-speed frontal crashes by comparing the upper neck loads to size-matched pediatric volunteers in similar loading environments. Previous studies have shown the HIII 10 and Q10 ATDs significantly underestimating axial loading (Seacrist et al. 2013). The LODC also underestimated axial loading of the upper neck but was closer to the human volunteers than the previous pediatric ATDs. This smaller underestimation shows improvement of the LODC in estimating the upper neck axial loading, helping to better predict pediatric cervical spine injury potential. Underestimation of axial loading at low speeds may be explained by the increased compliance of the human neck compared to the ATDs.

The LODC also displayed lower shear forces than the human volunteers. The HIII 10 and Q10 upper neck shear was closer to the human volunteers than the LODC. This shift from shear to axial force in the LOCD is likely due to the increased flexibility of the LODC spine, especially in the thoracic region. The LODC also underestimated upper neck bending moment compared to the human cohort while the HIII 10 was closer to the volunteer data. The LODC may be exhibiting less upper neck bending moment due to the increased flexibility of the thoracic spine, causing more rotation in the thoracic region and less at the head neck junction. The underestimation of bending moment also contributed in part to the LODC's underestimation of the neck injury criterion, N_{ij}.

The head angular acceleration of the LODC still slightly underestimated the volunteers but was substantially closer than the HIII 10 or Q10 ATDs. Unlike angular acceleration, the

LODC substantially overestimated both linear accelerations. The LODC also reach peak values of upper neck load variables slower than the HIII 10 and Q10 across the board. This is also a result of the increased flexibility of the thoracic spine due to the softer LODC spinal joints.

Several limitations of this study exist. The standard 3-point seat belt was not designed to resemble any specific automobile but instead sought to provide an automotive-like environment in which to compare human volunteers and ATDs. Previous studies have also shown that ATDs tend to exhibit lower excursions compared to PMHS at low speeds (Lopez-Valdes et al. 2010), thus cautioning the extrapolation of these data to higher impact scenarios. These findings may not be generalizable to higher loading rates (as seen in typical motor vehicle crashes) due to the viscoelasticity of the human spinal column. As continuous improvements are made upon ATDs, future work should continue to investigate the acceleration and loading of the pediatric ATDs in comparison the human volunteers. The additional flexibility of the thoracic spine of the LODC warrants further investigation.

CONCLUSIONS

This study furthers the evaluation of upper neck loading of multiple pediatric ATDs in comparison to human volunteer data. Specifically, the new LODC was analyzed alongside the HIII 10 and Q10 ATDs in comparison to a cohort of 9-11 year olds. In general, the LODC underestimated axial force, shear force, and bending moment about the upper neck, possibly due to the effects of softer joints and increased flexibility in the thoracic region of the spine. The LODC provided closer estimates to the human cohorts in shear force and head angular acceleration. The HIII 10 and Q10 ATDs provided closer estimates of axial force, bending moment, linear acceleration, and N_{ij} than the LODC. These analyses provide furthered insight to the biofidelity of the pediatric ATD upper neck loads in low-speed crash environments, specifically evaluating the improvements made upon the LODC.

ACKNOWLEDGEMENTS

REFERENCES

Arbogast KB, Jermakian JS, Ghati Y, Smith R, Menon RA, Maltese MR. Patters and predicors of pediatric head injury. Proc. International Research Council on The Biomechanics of Impact; Prague, Czech Republic. 2005.

Arbogast KB, Balasubramanian S, Seacrist T, et al. Comparison of kine- matic responses of the head and spine for children and adults in low- speed frontal sled tests. *Stapp Car Crash J.* 2009; 53:329–372.

Arbogast KB, Mathews EA, Seacrist T, et al. The effect of pre-tensioning and age on torso rollout in restrained human volunteers in far-side lateral and oblique loading. *Stapp Car Crash J.* 2012; 56:443–467.

Beeman SM, Kemper AR, Madigan ML, Franck CT, Loftus SC. Occupant kinematics in lojw-speed frontal sled tests: human volunteers, Hybrid III ATD, and PMHS. *Accid Anal Prev.* 2012; 47:128– 139.

Centers for Disease Control and Prevention. *WISQARS (Web-based Injury Statistics Query and Reporting System)*. Atlanta, GA: Author; 2013.

Irwin A, Mertz HJ. *Biomechanical Basis for the CRABI and Hybrid III Child Dummies*. Warrendale, PA: Society of Automotive Engineers; 1997. SAE Paper No. 973317.

Langhaar, Henry Louis. *Dimensional analysis and theory of models*. Vol. 2. New York: Wiley, 1951.

Menon, Rajiv, et al. *Evaluation of Restraint Type and Performance Tested with 3-and 6-year-old Hybrid III Dummies at a Range of Speeds*. No. 2004-01-0319. SAE Technical Paper, 2004.
Reed MP, Ebert-Hamilton SM, Klinich KD, Manary MA, Rupp JD. *Assessing Child Belt Fit, Volume I: Effects of Vehicle Seat and Belt Geometry on Belt Fit for Children With and Without Belt Positioning Booster Seats*. Ann Arbor, MI: University of Michigan, Transporta- tion Research Institute; 2008.

NHTSA. Federal motor vehicle safety standards, child restraint systems; Hybrid III 10-year old child test dummy. In: Supplemental Notice of Proposed Rulemaking (NHTSA-2010-0158-0001), 2010.

Seacrist T, Balasubramanian S, Garcia-Espana JF, et al. Kinematic comparison of pediatric human volunteers and the hybrid III 6-year-old anthropomorphic test device. *Ann Adv Auto Med.* 2010; 54:97–111.

Seacrist, Thomas, et al. "Kinematic comparison of the Hybrid III and Q-Series pediatric ATDs to pediatric volunteers in low-speed frontal crashes." *Annals of Advances in Automotive Medicine/Annual Scientific Conference*. Vol. 56. Association for the Advancement of Automotive Medicine, 2012.

Seacrist, T., A. B. Arbogast, M. R. Maltese, J. F. Garcı́a- Españ̃a, F. J. Lopez-Valdes, R. W. Kent, H. Tanji, K. Higuchi, and S. Balasubramanian. Kinetics of the cervical spine in pediatric and adult volunteers during low speed frontal impacts. J. Biomech. 45:99–106, 2012.

Seacrist, Thomas, et al. "Evaluation of the Hybrid III and Q-series pediatric ATD upper neck loads as compared to pediatric volunteers in low-speed frontal crashes." *Annals of biomedical engineering* 41.11 (2013): 2381-2390.

Seacrist, Thomas, et al. "Evaluation of pediatric ATD biofidelity as compared to child volunteers in low-speed far-side oblique and lateral impacts." *Traffic injury prevention* 15.sup1 (2014): S206-S214.

Stammen, Jason A., John H. Bolte IV, and Joshua Shaw. "Biomechanical Impact Response of the Human Chin and Manubrium." *Annals of biomedical engineering* 40.3 (2012): 666-678.

Viano, David C., et al. "Biomechanics of the human chest, abdomen, and pelvis in lateral impact." *Accident Analysis & Prevention* 21.6 (1989): 553-574.